Wireless Personal Communications **10:** 319–339, 1999.

Joint Data and Kalman Estimation for Rayleigh Fading Channels

M.J. OMIDI, S. PASUPATHY and P.G. GULAK
Department of Electrical and Computer Engineering, University of Toronto, Canada M5S 3G4
E-mail: omidi@eecg.toronto.edu

Abstract. Channel estimation is an essential part of many detection techniques proposed for data transmission over fading channels. For the frequency selective Rayleigh fading channel an autoregressive moving average representation is proposed based on the fading model parameters. The parameters of this representation are determined based on the fading channel characteristics, making it possible to employ the Kalman filter as the best estimator for the channel impulse response. For IS-136 formatted data transmission the Kalman filter is employed with the Viterbi algorithm in a Per-Survivor Processing (PSP) fashion and the ove rall bit error rate performance is shown to be superior to that of detection techniques using the RLS and LMS estimators. To allow more than one channel estimation per symbol interval, Per-Branch Processing (PBP) method is introduced as a general case of PSP and its effect on performance is evaluated. The sensitivity of performance to parameters such as fading model order and vehicle speed is also studied.

Keywords: fading channel, channel estimation, Kalman filtering, MLSE-based.

1. Introduction

Various kinds of Maximum Likelihood Sequence Estimation (MLSE) techniques are introduced in the literature to combat the degradation of error performance due to the severe ISI in fast fading channels. MLSE is usually implemented using the Viterbi algorithm. Generally all adaptive versions of MLSE receivers require some information about the fading channel such as estimates of the Channel Impulse Response (CIR) [1–4]. The quality of the channel estimation method has a strong impact on the overall Bit Error Rate (BER) performance of the receiver. Particularly in fast fading conditions, only the more advanced channel estimators can provide reasonable receiver performances.

An inherent difficulty associated with applying the estimation methods is that the unknown transmitted data is required for the estimator adaptation. In the "decision directed mode" the actual transmitted data, which is not available at the receiver a priori, is replaced by an estimate of the data stream. However, there is usually a decoding delay, namely a "decision delay" inherent in the Viterbi Algorithm, that causes poor tracking performance of conventional adaptive MLSE receivers on time varying channels. Moreover, channel estimation errors can lead to error propagation in these methods.

Per-survivor processing (PSP) is a sequence detection technique [3] in which the CIR is estimated along the surviving paths associated with each state of the trellis. Each surviving path maintains its own estimate of the channel based on the hypothesized transmitted data sequence. This method eliminates the decision delay and reduces the effects of error propagation, by embedding the data-aided estimation of the channel parameters into the structure of the Viterbi algorithm. However, PSP cannot be used with some estimation techniques if there are more than one channel estimation per symbol interval due to data dependency in the

implemented structure. In this paper we introduce the per-branch processing (PBP) method as a general case of PSP, which has the advantages of PSP and allows more than one estimation per symbol interval.

The performance of the receiver strongly depends on how well the estimator can track the rapid changes of the CIR in the fast fading conditions. Channel estimation is usually performed via LMS or RLS algorithms. However, the Kalman filter is the optimum estimation method that minimizes the estimation mean square error [5]. The Kalman filter is composed of two parts: *the measurement update equations* and *the time update equations*. The RLS algorithm is basically the same as the measurement update equations of the Kalman filter [6]. The state transition matrix used in the time update equations of the Kalman filter is not required in the RLS algorithm; and to implement the Kalman filter for achieving a better BER performance, some extra information about the state space model of the fading channel is required.

The application of the Kalman filter to the channel estimation of Rayleigh fading channels has been addressed by some authors [1, 7]; however, in these applications a relation between the parameters of the actual fading channel model and the state space model is not established. In this paper we propose a new method for obtaining an Autoregressive (AR) representation for the impulse response of the fading channel based on the fading model parameters. It will be shown that the state space model parameters can be easily obtained at the receiver by estimating the maximum Doppler frequency shift or equivalently finding the AR spectral estimation of CIR. This enables us to use the optimal Kalman filter consisting of both time and measurement updates for channel estimation, while in other approaches using RLS (also sometimes referred to as the Kalman algorithm) only measurement updates are posible at the estimator. In this method, the fading coefficients are obtained through an IIR filter. It is shown that the complexity of the Kalman filter depends on the order of the IIR filter and the trade-offs between the complexity and performance are studied. Although a two-ray fading channel is considered here, the complexity of this method and hence the complexity of the Kalman filter will not be affected by increasing the number of rays.

This paper is organized as follows: In Section 2, following a short overview of the mobile communication system under consideration, we present a model for the channel and derive the AR representation for the CIR. In Section 3, after introducing the estimation algorithms, we describe the proposed joint data and channel estimation method. After presenting the simulation results in Section 4, we conclude in Section 5.

2. Transmission System and The Channel Model

2.1. The Signal Model

To study a digital communication system over a frequency-selective Rayleigh fading channel we adopt the north American narrowband TDMA standard (IS-136), where the $\pi/4$-shifted differentially coded Quadrature Phase-Shift Keying (DQPSK) modulation technique is used. For simplicity we will consider the DQPSK signaling scheme instead, which should not lead to significant differences in performance. The complex baseband signal model for the communication system is shown in Figure 1. The complex data sequence $\{a_i\}$ with the symbol period T is input to the fading channel. Digital data signals are packed into TDMA blocks starting with a preamble training sequence. The training sequence helps the receiver to extract the necessary information about the channel. The data symbols are shaped in a raised-cosine shaping filter

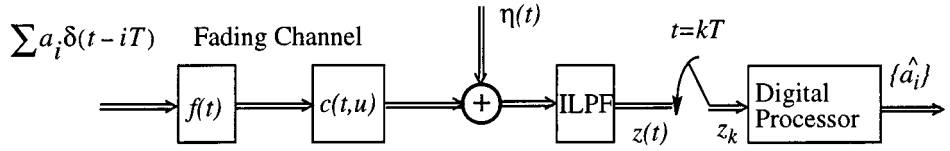

Figure 1. The signal model for the baseband communication system.

with impulse response $f(t)$ before transmission. The equivalent low-pass time-variant impulse response of the frequency-selective Rayleigh fading channel, $c(t, u)$, represents the channel response at time t due to an impulse applied at time $t - u$. The impulse response $c(t, u)$ is usually modeled as a wide-sense stationary uncorrelated scattering process. The additive noise $\eta(t)$ is a circularly symmetric [8] complex Gaussian process with power spectral density N. The bandwidth of the signal $z(t)$ is W and it is sampled at Nyquist rate ($T_s = 1/2W$). The noise samples $\eta(kT_s)$ are complex uncorrelated Gaussian random variables with variance $N_0 = 2WN$. In our treatment the channel impulse response (CIR) includes the impulse response of the cascade of the shaping filter, $f(t)$, and the fading channel, $c(t, u)$.

The receiver samples the incoming signal at the rate $1/T_s$ at the output of the low pass filter where $T = n_s T_s$, and n_s is the number of samples per symbol interval. By defining the information sequence at sampling times as

$$b_k = \begin{cases} a_{k/n_s} & \dfrac{k}{n_s} = \text{integer} \\ 0 & \text{otherwise} \end{cases} \tag{1}$$

the sampled signal, z_k, can be written as

$$z_k = \sum_{i=0}^{\beta} b_{k-i} h_{k,i} + n_k \,, \tag{2}$$

where $h_{k,i}$, the CIR at time k due to an impulse that was applied at time $k - i$, describes both $f(t)$ and $c(t, u)$ blocks of Figure 1 in the discrete time domain. In practical situations it is possible to truncate the CIR to a finite length and we assume its total length to be $(\beta + 1)$. The additive white Gaussian noise, n_k, represents $\eta(kT_s)$.

2.2. The Channel Model

Propagation in urban areas is mainly by way of scattering from the surfaces of the buildings and this makes a mobile communication channel a time varying multipath medium. In this multipath situation energy arrives via several paths simultaneously, and various incoming radiowaves arrive from different directions with different time delays. The impulse response of such a channel includes several pulses from different paths with different delays. Associated with each path is a time varying propagation delay and an attenuation factor. Here we will consider the simple case of a two-ray fading channel. The baseband impulse response at time t caused by an impulse applied at time u can be written as

$$c(t, t - u) = \alpha_0(u)\delta(t - u) + \alpha_1(u)\delta(t - u - \tau) \,, \tag{3}$$

where α_0 and α_1 are circularly symmetric Gaussian complex random coefficients. Figure 2 shows a model for this channel.

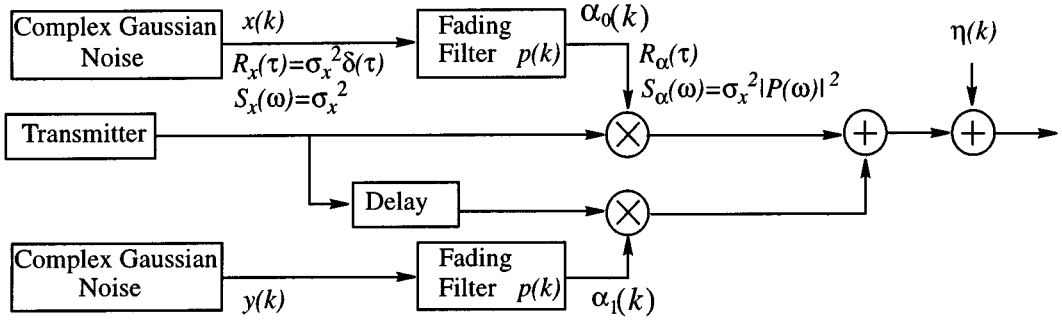

Figure 2. The fading channel model.

Simulation of the fading spectrum appropriate to mobile radio is obtained by choosing an appropriate characteristic for the two fading filters in Figure 2 and properly shaping the spectrum of the Gaussian noise processes. It is important to notice that although the spectrum of the Gaussian processes is affected by filtering, the probability density function is not, so the process at the output of the fading filter remains Gaussian. Theoretical spectral density of the complex envelope of the received signal is represented [9, 10] as

$$S(f) = \begin{cases} \dfrac{\varepsilon^2}{2\pi f_d}\left[1-\left(\dfrac{f}{f_d}\right)^2\right]^{-1/2} & |f| \le f_d \\ 0 & \text{elsewhere} \end{cases} \tag{4}$$

where ε is the rms value of the signal envelope and f_d is the maximum Doppler shift corresponding to the vehicle speed. As shown in Figure 2, complex Gaussian noise process is passed through a fading filter to create the multiplicative fading signal. The spectral density of the received signal envelope is determined by the transfer function of the fading filter, $P(\omega)$. To simulate the spectral density of (4), one must choose $P(\omega)$ proportional to the square root of $S(f)$. It is too difficult to design a filter whose output spectrum truly follows this shape, so an approximation has to be sought.

A fading filter with the impulse response $p(k)$ can be designed so that its output spectral density is an approximation to the square root of $S(f)$. The problem of designing a low order fading filter for shaping the spectral density of a white noise signal to be used as the complex envelope of the received signal in simulators is addressed in [11] and [12]. The proposed frequency response is a low pass characteristic with 0 dB gain at lower band, 6 dB peak at $f_p = f_d/r_f$, and –60 dB per decade slope after this frequency as shown in Figure 3. The r_f ratio can be chosen so that the fading filter transfer function curve is a close fit to the theoretical curve. By placing the peak point of $|H(f)|^2$ on the $S(f)$ curve we obtain $r_f = 1.03$. Implementation of this filter can be easily achieved by a third order fading filter. The transfer function of this filter in the z domain can be written as

$$P(z) = \frac{D}{1 - Az^{-1} - Bz^{-2} - Cz^{-3}}, \tag{5}$$

where the filter coefficients depend on f_d. If white Gaussian noise is applied to the input of the fading filter, the output envelope will have a Rayleigh distribution. To design this filter based on the constraints given in Figure 3, and to obtain the filter coefficients (A, B, C, and D), it is enough to estimate the maximum Doppler frequency shift $f_d = V/\vartheta$, where V is the vehicle

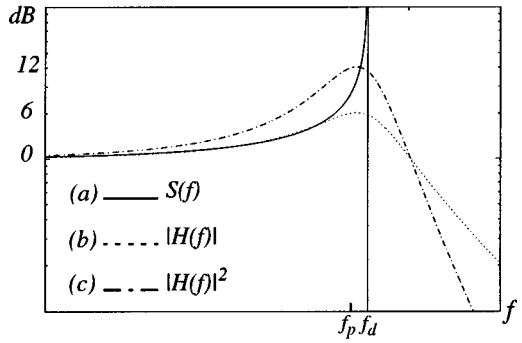

Figure 3. (a) Theoretical spectral density of the complex envelope of the received signal. (b) Fading filter frequency response, $|H(f)|$. (c) $|H(f)|^2$. ($f_p = f_d/1.03$).

speed and ϑ is the wavelength. The computer program of Appendix A can be used to calculate the fading filter coefficients given the maximum Doppler frequency f_d. In the following we will show that we can write an AR representation for the CIR based on the parameters of the fading filter. This will in turn help us to define the state space model parameters of the fading channel.

2.3. The AR Model for the CIR

Here we will derive an AR representation for the CIR based on the above fading channel model. In this context, the CIR is the impulse response of a system including both $f(t)$ and $c(t, u)$ (Figure 1). The response of the fading channel at discrete time k to an impulse applied at time j can be expressed as

$$c(k, k-j) = \alpha_0(j)\delta(k-j) + \alpha_1(j)\delta(k-j-\tau). \tag{6}$$

For the cascade of the shaping filter, $f(k)$, and the fading channel, $c(k, k-j)$, it can be verified that the response to $\delta(k-j)$, or $h_{k,k-j}$ is expressed as

$$h_{k,k-j} = \alpha_0(k) f(k-j) + \alpha_1(k-\tau) f(k-j-\tau) \tag{7}$$

and if we define $i = k - j$, (7) becomes

$$h_{k,i} = \alpha_0(k) f(i) + \alpha_1(k-\tau) f(i-\tau)\,. \tag{8}$$

On the other hand, from Figure 2 we can see that $\alpha_0(k)$ and $\alpha_1(k-\tau)$ are outputs of the fading filter and can be written as

$$\alpha_0(k) = x(k) * p(k) \tag{9}$$

and

$$\alpha_1(k-\tau) = y(k-\tau) * p(k)\,, \tag{10}$$

where $p(k)$ is the impulse response of the fading filter. Hence (8) becomes

$$h_{k,i} = [x(k) * p(k)] f(i) + [y(k-\tau) * p(k)] f(i-\tau) \tag{11}$$

or

$$h_{k,i} = [f(i)x(k) + f(i-\tau)y(k-\tau)] * p(k) \tag{12}$$

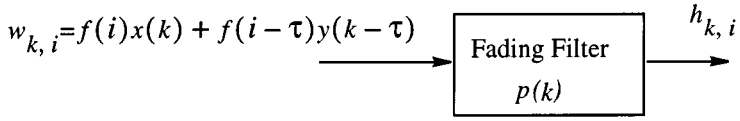

Figure 4. Illustration of the channel impulse response as the output of the fading filter.

and if we define

$$w_{k,i} = f(i)x(k) + f(i-\tau)y(k-\tau) \tag{13}$$

then

$$h_{k,i} = w_{k,i} * p(k). \tag{14}$$

Equation (14) suggests that the impulse response of the combination of shaping filter, and the fading channel, can be obtained at the output of the fading filter, if the input is the Gaussian noise process $w_{k,i}$, as shown in Figure 4. Here we have considered a two ray model; however, this result can be generalized to any number of rays. In a multi-ray condition CIR can be obtained as the output of the fading filter where the input is a sum of weighted Gaussian noise components, similar to the situation of Figure 4.

The CIR, $h_{k,i}$, is a wide-sense stationary Gaussian random signal and has an AR representation ([5] ch. 2). Using (14) and given the transfer function of the fading filter $P(z)$ as in (5), one can obtain the AR representation of the channel impulse response as

$$h_{k,i} = Ah_{k-1,i} + Bh_{k-2,i} + Ch_{k-3,i} + Dw_{k,i}\,. \tag{15}$$

This shows that the AR representation of the CIR directly depends on the fading filter characteristics. Also, assuming the third order fading filter of Figure 3, to have the fading filter coefficients one only requires to know the maximum Doppler frequency shift, f_d. This means if the receiver estimates f_d on a regular basis, like at the beginning of each data frame, it will have the AR representation of the CIR. In the following we will show that this AR model can be used to define the state space model of the fading channel.

In this model it is assumed that all rays experience the same fading spectrum. In reality, the shortest delay ray has the (long-term average) spectrum of (4), because the fading is typically due to a number of scatterers located close to and around the vehicle. However, the delayed rays are typically due to a large and distant scatterer (e.g., a large building, a cliff face, etc.) and are characterized by a much narrower spectrum. Nevertheless, in practical situations f_d is usually a small fraction of the symbol rate and the assumption that all rays have the same fading spectrum will not result in much loss. This assumption allows for the factorization shown in (11) and (12), leading to the AR representation of (15). An alternative approach to obtain the AR model of (15) for the CIR, is to employ one of the spectral estimation methods of ([13] ch. 6) to find the AR model parameters.

2.4. The State Space Model

To derive the state space model for the fading channel consider the $(\beta + 1)$ dimensional complex Gaussian random vector at sampling time k

$$\boldsymbol{h}_k = (h_{k,0}, h_{k,1}, \ \ldots, \ h_{k,\beta})^t\,, \tag{16}$$

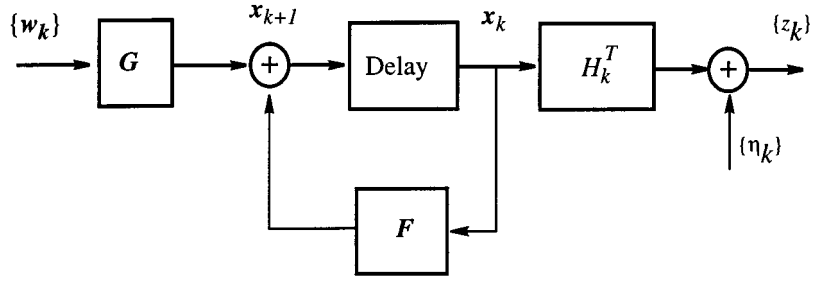

Figure 5. Linear time varying model of signal transmission over a Rayleigh fading channel.

where $(.)^t$ denotes matrix transposition. Using (15) we obtain

$$\boldsymbol{h}_k = A\boldsymbol{I}\boldsymbol{h}_{k-1} + B\boldsymbol{I}\boldsymbol{h}_{k-2} + C\boldsymbol{I}\boldsymbol{h}_{k-3} + D\boldsymbol{I}\boldsymbol{w}_k\,, \tag{17}$$

where $\boldsymbol{I}$ is a $(\beta+1)\times(\beta+1)$ unit matrix. The vector $\boldsymbol{w}_k$ is a $(\beta+1)\times 1$ zero mean white Gaussian process with the covariance matrix defined as $E\{\boldsymbol{w}_k\boldsymbol{w}_l^T\} = \boldsymbol{Q}\delta_{kl}$. According to (17), $\boldsymbol{h}_k$ only depends on its three past values; and if we define the states of the state-space model as a vector composed of 3 consecutive impulse responses

$$\boldsymbol{x}_k = (\boldsymbol{h}_k, \boldsymbol{h}_{k-1}, \boldsymbol{h}_{k-2})^t \tag{18}$$

then using (17) and (18) we can write

$$\boldsymbol{x}_{k+1} = \begin{bmatrix} A\boldsymbol{I} & B\boldsymbol{I} & C\boldsymbol{I} \\ \boldsymbol{I} & 0 & 0 \\ 0 & \boldsymbol{I} & 0 \end{bmatrix} \boldsymbol{x}_k + \begin{bmatrix} D\boldsymbol{I} \\ 0 \\ 0 \end{bmatrix} \boldsymbol{w}_k \tag{19}$$

or

$$\boldsymbol{x}_{k+1} = \boldsymbol{F}\boldsymbol{x}_k + \boldsymbol{G}\boldsymbol{w}_k \tag{20}$$

where $\boldsymbol{F}$ and $\boldsymbol{G}$ are $3(\beta+1)\times 3(\beta+1)$ and $3(\beta+1)\times(\beta+1)$ matrices respectively. $\boldsymbol{F}$ is called the state transition matrix and $\boldsymbol{G}$ is the process noise coupling matrix.

The $3(\beta+1)\times 1$ vector $\boldsymbol{H}_k$ can be defined as

$$\boldsymbol{H}_k = (b_k, b_{k-1}, b_{k-2}, \ \ldots,\ b_{k-\beta}, 0, \ \ldots,\ 0)\,, \tag{21}$$

where $2\times(\beta+1)$ zeros are inserted after $b_{k-\beta}$. The received signal can be expressed by

$$z_k = \boldsymbol{H}_k\boldsymbol{x}_k + n_k\,. \tag{22}$$

Equations (20) and (22) describe the linear time varying system of Figure 5 where $\boldsymbol{x}_k$ is the state vector of this system, $\boldsymbol{H}_k$ is called the measurement matrix and the received signal z_k can be assumed to be a noisy measurement of the states of the system.

As mentioned before, the covariance matrix of the Gaussian noise process $w_{k,i}$ is $E\{\boldsymbol{w}_k\boldsymbol{w}_l^T\} = \boldsymbol{Q}\delta_{kl}$, where $(.)^T$ denotes Hermitain transpose, and the matrix $\boldsymbol{Q}$ can be obtained using (13). The element on the ith row and the jth column of $\boldsymbol{Q}$ is

$$q_{ij} = E\{w_{k,i}w_{k,j}\} \tag{23}$$

or

$$q_{ij} = E\{[f(i)x(k) + f(i-\tau)y(k-\tau)]\times[f(j)x(k) + f(j-\tau)y(k-\tau)]\}.$$

The $x(k)$ and $y(k)$ signals are white processes with variances σ_x^2 and σ_y^2, therefore q_{ij} is zero for $i \neq j$ and for the diagonal elements of $\boldsymbol{Q}$ we obtain

$$q_{ii} = \sigma_{w_{k,i}}^2 = f^2(i)\sigma_x^2 + f^2(i-\tau)\sigma_y^2 \,. \tag{24}$$

Having defined the parameters of the state space model, we are ready to employ an estimation method for estimating the states of the system or the impulse response of the channel.

2.5. Parameter Estimation Using The Received Signal

In practice, for some channel estimation algorithms, it is necessary to extract the required channel state space model parameters from the received signal. The parameters of the fading filter in (5) are used to generate $\boldsymbol{F}$ and $\boldsymbol{G}$ and an estimation of these parameters is required at the receiver. Also the matrix $\boldsymbol{Q}$ and the noise variance N_0 need to be calculated for the implementation of the Kalman filter.

To obtain $\boldsymbol{F}$ and $\boldsymbol{G}$, we need to find the AR model parameters of (15). The estimated state vector at the receiver, $\hat{\boldsymbol{x}}_k$, consists of the estimates of CIR taps, $\hat{h}_{k,i}$, (see (16), (18)). The process $\hat{h}_{k,i}$ is characterized by the AR model of (15). There are several spectral estimation methods ([13] ch. 6) that can be employed to find these AR model parameters. The AR spectral estimation provides the parameters of $\boldsymbol{F}$ and $\boldsymbol{G}$ and the variance of the AR model noise. As mentioned earlier, assuming the filter characteristics of Figure 3, estimating the AR parameters for the CIR is equivalent to finding the maximum Doppler frequency shift. Hereafter, we refer to this AR spectral estimation as the estimation of maximum Doppler frequency shift.

To obtain $\boldsymbol{Q}$ we notice that it is a diagonal matrix as defined in (24). The diagonal elements are the variance of the AR model noise, $\sigma_{w_{k,i}}^2$, and can be obtained in the process of spectral estimation techniques of [13]. The additive noise variance N_0 can be estimated based on a comparison of the detected sequence and the received signal.

In the next section after introducing the Kalman filter and the RLS algorithm we will consider their implementation in a MLSE-VA receiver.

3. Joint Data and Channel Estimation

3.1. The Kalman Filter

The Kalman filter is an optimal linear minimum variance estimator. It can provide real-time estimates of the states of a system from noisy measurements. The Equations (20) and (22) describe a linear system and form a Kalman filtering problem. The algorithm given in Table 1 is well known for the Kalman Filter [5]. The estimate of $\boldsymbol{x}_k$ is $\hat{x}_k$ and $\boldsymbol{P}_k$ is the error covariance matrix of state estimates.

The Kalman filter is a recursive algorithm composed of two parts: *Measurement Update Equations* and *Time Update Equations*. Using the measurement update equations, the Kalman filter estimates the next state vector of the linear system or the CIR based on a noisy measurement which is the input signal at the receiver. Then, using the time update equations, the Kalman filter updates its estimate of the next state vector according to its knowledge of the linear system parameters such as $\boldsymbol{F}$ and $\boldsymbol{G}$.

Table 1. The Kalman filter and RLS algorithms.

The Kalman filter algorithm l	The RLS algorithm
Minimizes the estimation mean square error:	Minimizes the cost function:
$E\{(x-\hat{x})^T(x-\hat{x})\}$	$\xi(i)=\sum_{k=1}^{i}\lambda^{i-k}\lvert z_k-\boldsymbol{H}_k\hat{\boldsymbol{x}}_k\rvert^2$
Measurement update equations:	
$\hat{\boldsymbol{x}}_{k\lvert k}=\hat{\boldsymbol{x}}_k+\boldsymbol{K}_k(z_k-\boldsymbol{H}_k\hat{\boldsymbol{x}}_k)$	$\hat{\boldsymbol{x}}_{k+1}=\hat{\boldsymbol{x}}_k+\boldsymbol{K}_k(z_k-\boldsymbol{H}_k\hat{\boldsymbol{x}}_k)$
$\boldsymbol{K}_k=\boldsymbol{P}_k\boldsymbol{H}_k^T R_k^{-1}$	$\boldsymbol{K}_k=\boldsymbol{P}_k\boldsymbol{H}_k^T R_k^{-1}$
$R_k=\boldsymbol{H}_k\boldsymbol{P}_k\boldsymbol{H}_k^T+N_0$	$R_k=\boldsymbol{H}_k\boldsymbol{P}_k\boldsymbol{H}_k^T+\lambda$
$\boldsymbol{P}_{k\lvert k}=\boldsymbol{P}_k-\boldsymbol{K}_k\boldsymbol{H}_k\boldsymbol{P}_k$	$\boldsymbol{P}_{k+1}=\lambda^{-1}(\boldsymbol{P}_k-\boldsymbol{K}_k\boldsymbol{H}_k\boldsymbol{P}_k)$
Time update equations:	
$\hat{\boldsymbol{x}}_{k+1}=\boldsymbol{F}\hat{\boldsymbol{x}}_{k\lvert k}$	
$\boldsymbol{P}_{k+1}=\boldsymbol{F}\boldsymbol{P}_{k\lvert k}\boldsymbol{F}^T+\boldsymbol{G}\boldsymbol{Q}\boldsymbol{G}^T$	

3.2. The RLS Algorithm (Kalman Algorithm)

The RLS algorithm [14] is a least squares method to minimize the cost function with exponential weighting as given in Table 1. The parameter λ is a forgetting factor and from (22) we can see that $z_k-\boldsymbol{H}_k\hat{\boldsymbol{x}}_k$ is the noise component at the receiver according to the estimates of the channel impulse response. Using this cost function the estimator tries to estimate $\hat{\boldsymbol{x}}_k$ so that $\boldsymbol{H}_k\hat{\boldsymbol{x}}_k$ is as close as possible to the received signal plus noise.

By comparing the Kalman filter and the RLS algorithm, we observe that the RLS algorithm is basically the same as the measurement update equations of the Kalman filter. The RLS estimator uses the information of the received signal to update its state estimates and the estimation is performed in one stage similar to the measurement update equations of the Kalman filter. The Kalman filter performs some extra computations using the time update equations. The Kalman filter uses its knowledge about the linear system, obtained from the matrixes $\boldsymbol{F}$ and $\boldsymbol{G}$, and updates the estimated values once more. Hence, when we do not have enough information about the channel system (i.e. matrices $\boldsymbol{F}$, $\boldsymbol{G}$ and $\boldsymbol{Q}$, and N_0), the RLS algorithm is a good choice and when the channel parameters are known we can implement the Kalman filter which is the optimal estimator. To obtain the matrices $\boldsymbol{F}$ and $\boldsymbol{G}$ the receiver has to estimate the maximum Doppler frequency shift, and calculate the fading filter parameters of (5) based on this estimation. Since the changes in the vehicle speed are not very fast, the estimation of f_d can be made off-line and once for every block or every few blocks of data.

3.3. Data Sequence Estimation with PBP and PSP

MLSE is usually implemented via the Viterbi algorithm and in the case of an unknown channel, an estimate of the CIR is required at the receiver. Both of the above estimation methods require the vector $\boldsymbol{H}_k$, which is defined in (21) and depends on the transmitted data sequence. However, the transmitted data is not available at the receiver. This problem is sometimes

called "state estimation with model uncertainty", where the channel estimator has to estimate the states of the linear system of Figure 5 and the vector $\boldsymbol{H}_k$, is unknown.

A solution to this problem is proposed in [3] to implement the channel estimation in the Viterbi algorithm in a Per-Survivor Processing (PSP) fashion. In this paper we are introducing the Per-Branch Processing (PBP) method as a generalized form for PSP. The PBP method can be used when there are more than one channel estimation per symbol interval. Here, we will discuss the general method of per-branch processing for more than one channel estimation per symbol and we will show that in the special case of one sample per symbol it can be reduced to the PSP method.

Consider the application of the Viterbi algorithm for detecting a transmitted data sequence over a Rayleigh fading channel. The received signal samples, z_k, are used to compute the branch metrics for all of the branches in the trellis diagram. The Euclidean distance is a suitable branch metric when noise is Gaussian with constant variance

$$BM = |z_k - \boldsymbol{H}_k \hat{\boldsymbol{x}}_k|^2 \tag{25}$$

and when the noise variance is not constant the log-likelihood branch metrics are used

$$BM = \frac{|(z_k - \boldsymbol{H}_k \hat{\boldsymbol{x}}_k)|^2}{\sigma_k^2} + \log(\sigma_k^2)\,, \tag{26}$$

where σ_k^2 is the time varying noise variance and can be obtained as a by-product of the Kalman filter (R_k) used for channel estimation. To overcome the problem of uncertainty in $\boldsymbol{H}_k$, on each branch of the trellis a hypothesized data vector, $\boldsymbol{H}_k$, will be chosen according to the state transition corresponding to that branch. Then a separate estimator is required for any of the hypothesized $\boldsymbol{H}_k$ vectors on each branch. The computational procedure of the PBP method for three samples per symbol interval is shown in Figure 6. The computation is on a branch between states S_i and S_j. There are three received samples (Z) and three hypothesized data vetors ($\boldsymbol{H}$) on this branch. After receiving the first received signal sample, a Branch Metric Generator (BMG) unit obtains a measure of the likelihood of the hypothesized data vector, given the received sample, as in (25) or (26). At the same time an Estimator unit updates the channel estimates based on the received signal and the hypothesized $\boldsymbol{H}$. The new estimates will be passed to an accumulative BMG and another estimator to be processed with the second received sample and hypothesized $\boldsymbol{H}$. After processing all three samples in three stages, as shown in the figure, the branch metric is ready and the procedure of Add-Compare-Select can be started at node S_j to find the survivor branch. Similar to the regular Viterbi algorithm the information of the survivor path to each node has to be stored. Moreover, the estimated CIR on the survivor path will be used as the initial value for the estimators on the outgoing branches from that node. Since the same routine has to be performed on all of the branches of the trellis diagram it is called PBP.

The procedures required to perform the PBP algorithm are summarized in Figure 7(a). The boxes represent the channel estimation on each branch and the bold lines represent the channel estimates on the survivor paths that are passed to the outgoing branches. The PBP algorithm can be performed in four steps as shown in Figure 7(a). First the channel estimations have to be performed and then the branch metrics can be computed. After finding the survivor path only the estimates along this path will be retained and passed to the next stage as the initial values.

In this way, the estimators on each branch use their own hypothesized data vector for $\boldsymbol{H}_k$ and based on that, they update the estimates of the CIR. Here, on each branch instead

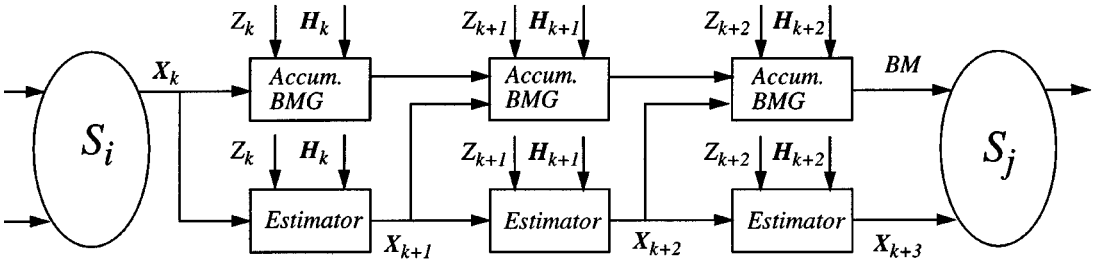

Figure 6. Data flow for the computations required on each branch of the trellis in PBP.

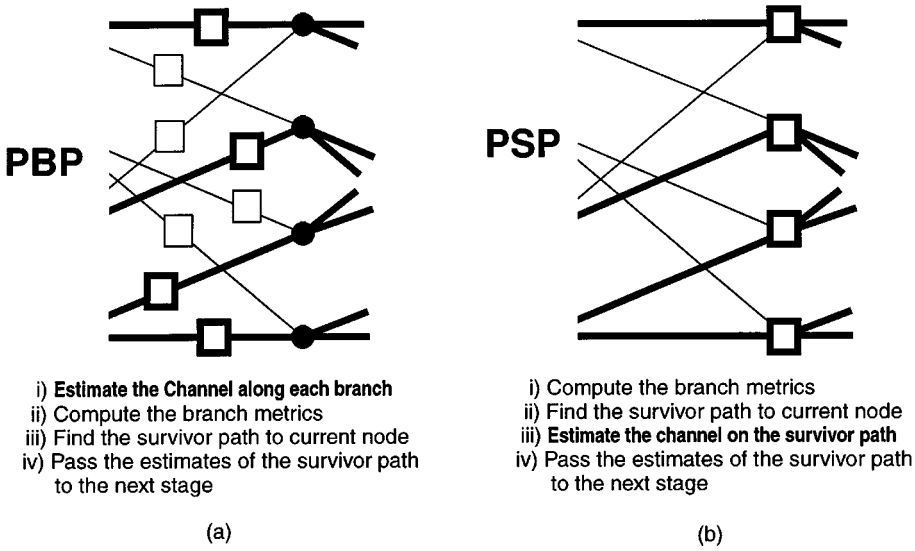

Figure 7. The PBP and PSP algorithms.

of a delayed data sequence, a hypothesized data vector corresponding to the state transition on that branch is used. This guarantees that we are using the data sequence of the shortest path for the channel estimation along the same path, which is obviously the best available information at the receiver. This method also eliminates the problem of decision delay, since the detected data associated with each survivor path is used for channel estimation on the same path immediately.

In the simple case of one sample per symbol interval, Figure 6 reduces to Figure 8(a) in which only one estimator and one BMG unit are used. In this case it is possible to reduce the complexity and avoid unnecessary estimations. The channel estimations on all of the branches can be postponed and first the branch metrics are computed and the Add-Compare-Select procedures are performed to find the survivor branch to each node. Then only the estimators on the surviving paths will be used to update the channel estimates for the next symbol interval. In this case only the estimators on the survivor paths are used and this is equivalent to having one estimator for each state in the trellis instead of each branch, as in Figure 8(b). This method is called PSP, where the number of estimations is reduced to the number of surviving paths and can be considered as a special case of PBP.

Figure 7(b) shows the procedures required to perform the PSP algorithm. Estimators are moved to the nodes from branches and hence a smaller number of estimators is required. By comparing the four steps that are required for PSP to that of PBP, we can realize that channel

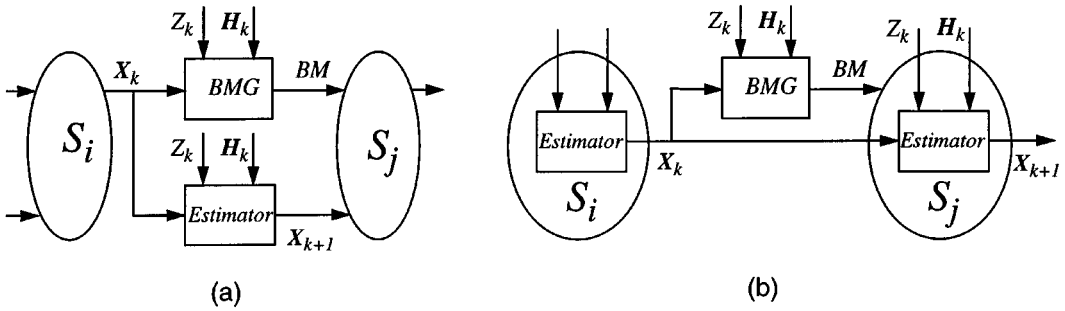

Figure 8. (a) Data flow for PBP with one sample per symbol interval, which can be reduced to PSP. (b) Data flow for PSP equivalent to (a).

estimation is postponed to the third step and is restricted to the surviving paths. It should be noted that in the previous case (Figure 6) with more than one sample per symbol, because of the data dependency it was not possible to postpone the channel estimations until the branch metrics are ready and the survivor path is known. By studying the data dependency on this diagram we can realize that only the last estimation could be deferred in this case.

On fast fading channels, the error floor in the BER curve can be appreciably lowered if more than one sample of the received signal is processed at the receiver [15, 16]. In a fast fading channel one sample per symbol interval is no longer a sufficient statistic for the decision process. Therefore, the number of samples per symbol can be increased to attain the sufficient statistics and to allow for more channel estimations per symbol interval; which results in a better tracking performance and a more accurate channel estimation at the receiver. However, more samples per symbol interval demand more signal processing and faster hardware for implementation. With the advent of the VLSI technology the implementation of high speed and parallel signal processing algorithms has become more feasible and the implementation of complex estimation and detection techniques such as the Kalman based PBP will be affordable with reasonable cost.

Any channel estimation algorithm, can be utilized in the above joint channel estimation and data detection methods. The difference in the results will be due to the tracking performance and precision of the estimators. By using the channel model of Section 2, it is possible to employ the Kalman estimator which is the optimal estimation method and, as is shown in the next section, its performance is superior to that of other estimators.

As mentioned before, by approximating the spectral density of the complex envelope of the received signal and considering a lower order fading filter as in (5), we can find an AR representation for the channel impulse response, and obtain the matrices $\boldsymbol{F}$ and $\boldsymbol{G}$ as described in (19) and (20). The time update equations of the Kalman filter, which provides the basic advantage of this estimator over the RLS algorithm, can be implemented using these matrices. The matrices $\boldsymbol{F}$ and $\boldsymbol{G}$ form the knowledge of the receiver about the fading channel and their components are determined by the parameters of the IIR fading filter of (5).

It should be noted that the proposed receiver scheme can be used for a multi-ray channel as long as we assume the same length for the channel impulse response. Although we have assumed a two ray fading channel in our simulations, the structure of the receiver and its complexity will not change if there is a larger number of rays in the channel. The only difference will be in the computation of the covariance matrix elements of (24), and other parameters will be unaffected.

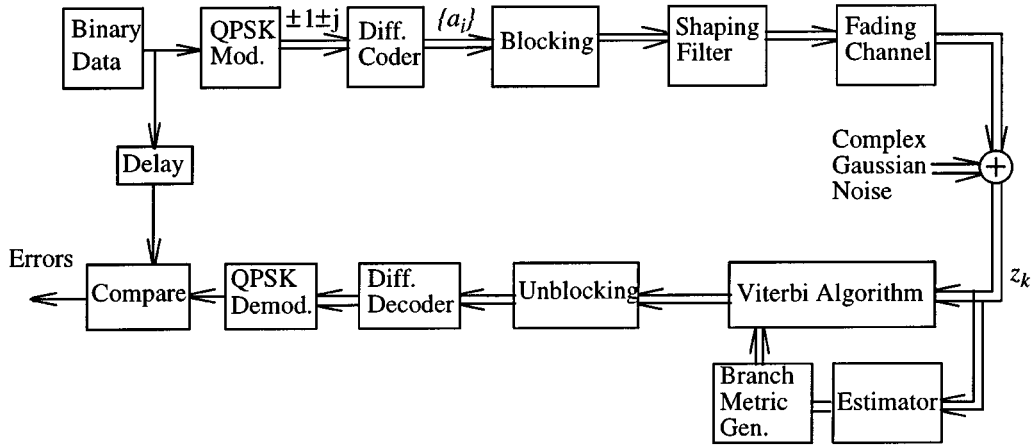

Figure 9. Block diagram of the simulation system.

In the next section, we present the simulation results where the effect of using the Kalman filter on lowering the bit error rate is studied.

4. Simulation Results

In the computer simulations, the modulation scheme employed is differentially coherent QPSK, with a symbol rate of 25 ksymbol/s, which is a little higher than 24.3 ksymbol/s in the IS-136 standard. A detailed block diagram of the simulated system is shown in Figure 9. As in the IS-136 standard, the differentially encoded data sequence is arranged into 162 symbol frames. The first 14 symbols of each frame is a training preamble sequence to help the adaptation of the channel estimator. For the shaping filter $f(t)$ at the transmitter, we implement an FIR filter which approximates a raised cosine frequency response. The fading channel is simulated as a symbol-spaced two-path model with time varying complex coefficients. The two fading paths are independent with equal strength, and are implemented as shown in the model of Figure 2. The receiver takes 3 samples per symbol interval and the complex samples are processed by the digital processor to detect the transmitted data. Differential encoding and differential detection enables the receiver to avoid errors due to phase ambiguity.

There is no intersymbol interference for the transmitted symbols at the transmitter[1] and the ISI at the receiver is due to the multipath nature of the channel. The total length of the channel impulse response is 2 symbol intervals and there are four possible states in the trellis diagram of the Viterbi algorithm at the receiver. For each state in the trellis there are four possible transitions to the four states in the next stage.

Figure 10 shows the simulation results for a vehicle speed of 100 km/h. The BER performance of different estimators are compared here at different values of E_b/N_0, where E_b is the average bit energy. In each simulation different channel estimators are used to estimate the channel impulse response on every received sample. From the results, it can be observed that the performance of the RLS algorithm is superior to that of LMS algorithm by about 3 dB at a BER $= 10^{-3}$. This is due to the faster tracking behavior of the RLS algorithm in the fast fading

[1] The discrete impulse response of the shaping filter has a finite length, equal to the symbol interval and hence does not produce ISI; the samples for the given roll off factor of 25% were obtained using the SPW^{TM} software package.

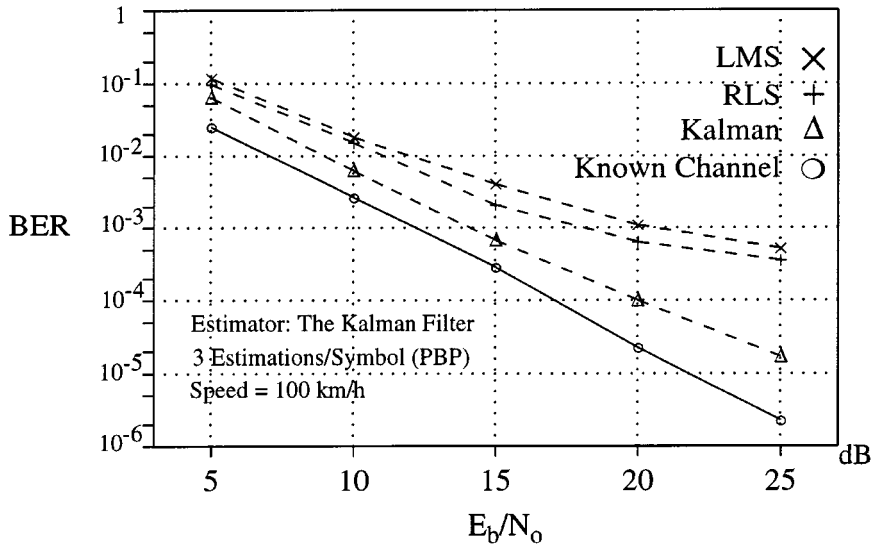

Figure 10. Simulation results with different estimation methods.

conditions. Choosing the Kalman estimator provides 7 dB improvement in performance over the LMS algorithm at the same BER, and it shows the superiority of this estimation method over the LMS and RLS algorithms.

The last curve is for the case of data detection over a known channel. In this case we have assumed that the exact channel impulse response is always known to the receiver and there is no need to estimate it. Of course this situation is not possible in a practical implementation, and this can be viewed as an error-free estimation method giving a lower BER bound for comparison. The performance of the Kalman filter is about 2 dB poorer than the best possible results obtained with a known channel at a BER $= 10^{-3}$.

When the channel impulse responsed does not change very rapidly, the channel estimation can be performed at a lower rate. This leads to less computation at the receiver. Figure 11 compares the results for the Kalman estimator for the situation of one channel estimation every symbol interval using the PSP method and the situation of three channel estimations per symbol interval using PBP. As we can see there is a difference of about 2 dB at a BER $= 10^{-4}$ between the two methods, which in some cases, might be tolerated to reduce the complexity of the receiver.

As mentioned before, to employ the Kalman filter estimator the receiver computes the matrices $\boldsymbol{F}$ and $\boldsymbol{G}$ based on its assumption about the maximum Doppler frequency shift. In Figure 12 we can observe the effect of error in the estimation of the maximum Doppler frequency shift. The curve labeled 100S-100E is for the normal case where the actual speed of the vehicle is 100 km/h and it is correctly assumed as 100 km/h in the receiver. The curves 150S-100E and 50S-100E show the situation where the actual speed is 150 and 50 km/h, respectively, but in both cases the speed is assumed to be 100 km/h at the receiver. And finally for the 50S-50E curve the receiver assumes the correct speed for a vehicle with the speed of 50 km/h.

In Figure 12 the dashed lines show the situation when the estimate of the vehicle speed is in error by 50 km/h and in both cases the performance is about 2 to 4 dB poorer than the case where we assume the correct speed for the vehicle. It can be easily observed that

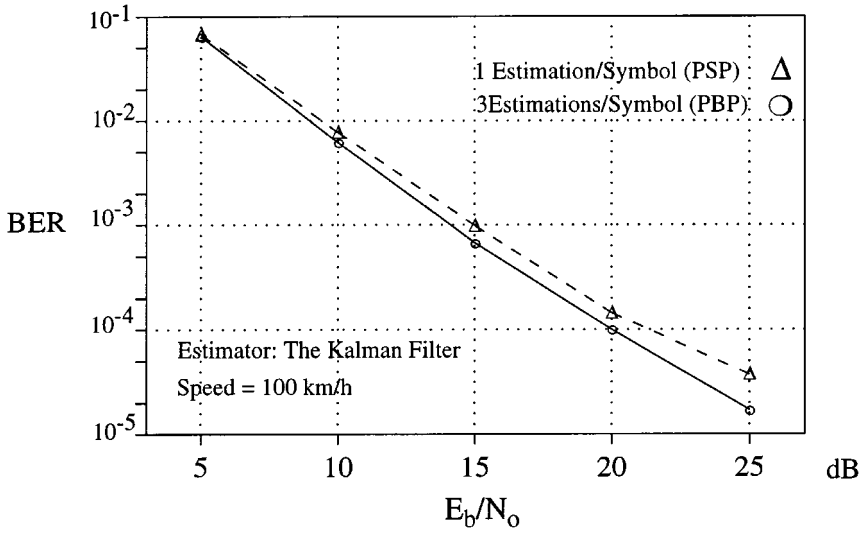

Figure 11. The result of changing the estimation rate for the Kalman estimator.

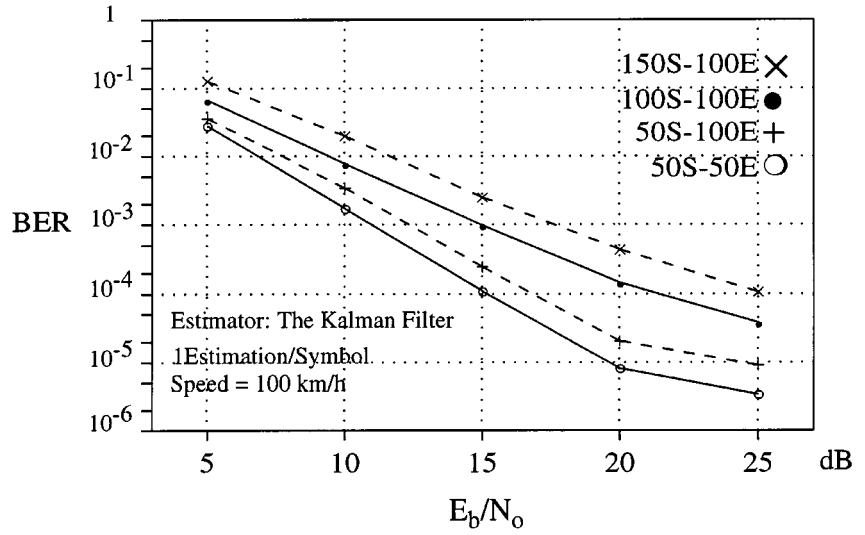

Figure 12. The effect of error in estimation of Doppler frequency shift, using the Kalman Filter.

we can always attain better results than what we are expecting by overestimating the speed. By accepting a reasonable margin in BER performance, one may assign a limited number of speeds and switch from one preselected speed threshold to another when the vehicle speed changes.

To reduce the complexity of the receiver we may consider a lower order fading filter at the receiver. In this case the dimensions of the matrix $\boldsymbol{F}$ will decrease and it mitigates the computational burden of time update equations of the Kalman filter. Figure 13 shows the results for this case, where the channel is simulated with a third order fading filter as before, and the receiving filter is assumed to have a lower order. In Figure 13 the results for the case of second order and first order fading filters are compared to that of a third order filter. The second order filter has been designed to have 6 dB overshoot at the maximum doppler frequency shift.

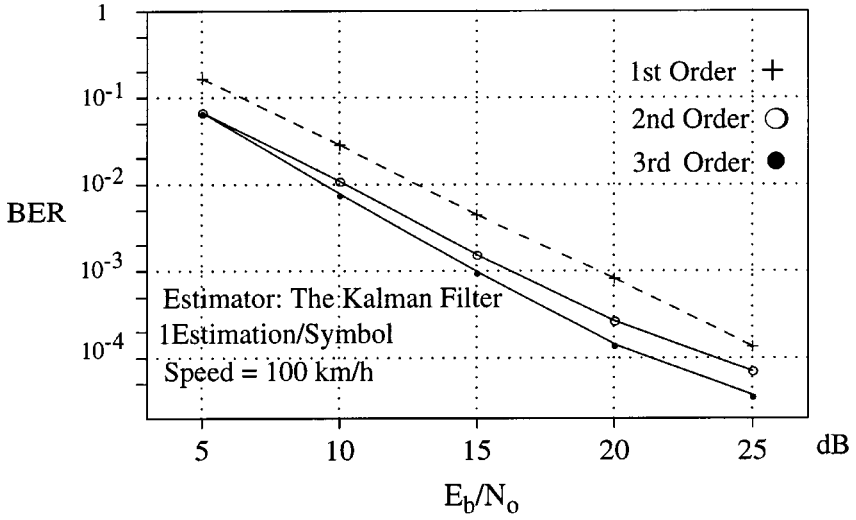

Figure 13. The effect of considering lower order fading filters at the receiver.

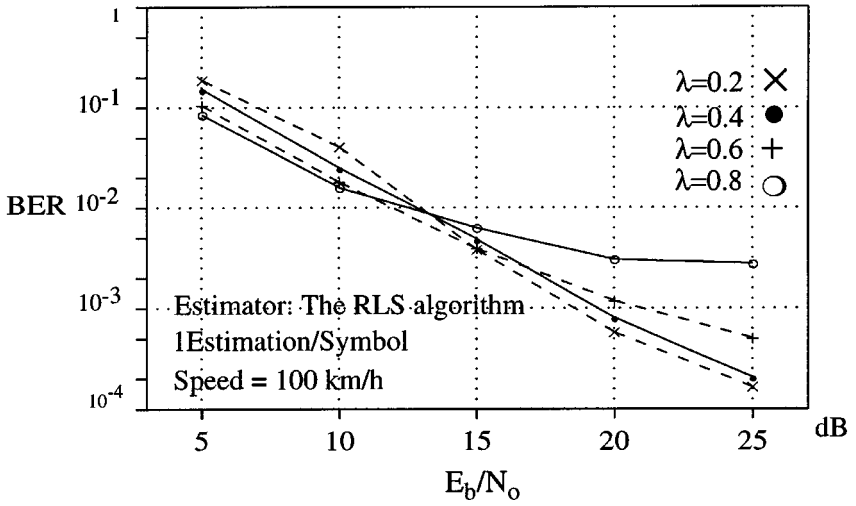

Figure 14. The effects of changing λ in the RLS algorithm on the overall BER performance.

In this case the parameter C in (5) will be eliminated and this results in smaller dimensions for the matrices and vectors in the receiving algorithm.

For the first order filter, it was realized that the performance of the receiver is very sensitive to the choice of cut-off frequency. By keeping the cut off frequency close to that of the second order filter attempts were made to find the optimum cut off frequency that leads to the best BER performance. It was observed that without a proper cut off frequency for the first order fading filter the time update equations of the Kalman filter seem to have negligible effect and we obtain a BER performance very close to the case of using the RLS algorithm, where the time update equations are absent.

In the RLS algorithm the overall BER performance depends on the chosen value for the forgetting factor, λ. Figure 14 shows the BER curves for different values of λ. It can be seen that for small E_b/N_0, larger values of λ yield better results, while for high E_b/N_0 values, λ should be smaller.

The RLS algorithm minimizes its cost function over an interval which is determined by λ. The above consequence means that in poor E_b/N_0 conditions the estimator should consider a larger interval to minimize the cost function, while for high E_b/N_0 values minimization over smaller intervals yields better performance.

It was observed that the results with the RLS algorithm for the case of one estimation per symbol are very close to what is given in [2] for $k = 1$, and it is possible to improve the performance by applying the Kalman filter. From the above results, the superiority of the Kalman filter is clearly evident. The Kalman filter shows the best tracking performance for rapidly changing time-variant channels, followed by the RLS algorithm as the next best choice as a good estimator with fast tracking. However, in spite of their superior tracking performance, the Kalman filter and the RLS algorithm have two disadvantages. One is the sensitivity of these recursive algorithms to round-off noise. This may cause numerical instabilities such that the algorithm may diverge due to round-off noise if the word-length is not long enough in the DSP implementation. The second problem is the complexity of these algorithms that originates from the iterative processing of the matrix operations. Square root filtering, implemented in the form of VLSI systolic architectures can be used to combat the problem of numerical instability and complexity of the Kalman filter and the RLS algorithm [17–19].

5. Conclusions

In this paper we derived an AR representation for the CIR in the frequency selective Rayleigh fading channel. A relation is established between the fading channel model and its state space model parameters, which allows the implementation of the Kalman filter as the optimum channel estimation technique. It is shown that the required information to implement the Kalman filter can be obtained by AR spectral estimation of the estimated CIR. PBP was introduced as a generalization for PSP to be used for more than one channel estimation per symbol interval. The differences between PBP and PSP were pointed out.

The BER results with the Kalman estimator were shown to be superior to that of other estimation methods. It was important to have a correct estimate of the vehicle speed. By considering the effects of error in speed estimation, we concluded that it is always better to overestimate the vehicle speed. Lower order fading filters were used to simplify the receiver structure, however, the first order filter was realized to be very sensitive to the choice of cut off frequency.

In the RLS algorithm choosing a proper value for the forgetting factor, λ, was considered. For low signal-to-noise ratios it was better to choose values close to one for λ, and for high signal-to-noise ratios the value of λ should be kept small.

Appendix

The following Matlab program is used to design the fading filter and generate the coefficients of (5). The filter is a cascade of a second order filter with 9 dB peak at Wmax and a first order filter with –3 dB gain at this frequency. The result will be a third order filter with 6 dB peak at Wmax. The inputs of the program are the *speed* of the vehicle in m/sec, sampling frequency in Hz, and the radio propagation frequency fp in Hz.

function$[A, B, C, D]$ = fadefilt(speed, Samp_freq, fp)

$fm = v/(3e8/fp)$; % Maximum Doppler Frequency
$rf = 1.03$;
$W\max = 2 * pi * (fm/rf)$;
$Q = 2.7823834$; % Q is chosen to yield a 9 dB peak
$Wo = W\max/(\text{sqrt}(1 - 1/(2 * Q\hat{}2)))$;
% Poles of the second order in s domain
$s1 = Wo/(2 * Q) + Wo * (\text{sqrt}(1 - 1/(4 * Q\hat{}2))) * 1i$;
$s2 = Wo/(2 * Q) + Wo * (\text{sqrt}(1 - 1/(4 * Q\hat{}2))) * 1i$;

% Second order filter coefficients
$A2 = 2 * \exp(-\text{real}(s1)/\text{Samp\_freq}) * \cos(\text{abs}(\text{imag}(s1)\text{Samp\_freq}))$;
$B2 = -\exp(-\text{real}(s1)/\text{Samp\_freq})\hat{}2$;
$D2 = 1 - A2 - B2$;

% First order filter coefficients
$A1 = \exp(-W\max/\text{Samp\_freq})$;
$D1 = 1 - A1$;

% Third order filter coefficients
$A = A2 + A1$;
$B = B2 - A2 * A1$;
$C = -B2 * A1$;
$D = -D1 * D2$;

Acknowledgements

The authors wish to thank an anonymous reviewer for a careful review and insightful comments, which have been included in the last paragraph of Section 2.3 of this paper.

This research was supported by Information Technology Research Centre (ITRC), a centre of excellence, funded by the province of Ontario, Canada.

References

1. Q. Dai and E. Shwedyk, "Detection of Bandlimited Signals over Frequency Selective Rayleigh Fading Channels", IEEE Transaction on Communications, Vol. 42, pp. 941–950, 1994.
2. J. Lin, F. Ling and J.G. Proakis, "Joint Data and Channel Estimation for TDMA Mobile Channels", International Journal of Wireless Information Networks, Vol. 1, No. 4, pp. 229–238, 1994.
3. R. Raheli, A. Polydoros and C. Tzou, "Per-Survivor Processing: A General Approach to MLSE in Uncertain Environments", IEEE Transaction on Communications, Vol. 43, pp. 354–364, 1995.
4. R. Fukawa and H. Suzuki, "Adaptive Equalization with RLS-MLSE for Frequency-Selective Fast Fading Mobile Radio Channels", Globecom '91, pp. 16.6.1–16.6.5, 1991.
5. B.D.O. Anderson and J.B. Moore, "Optimal Filtering", Prentice-Hall, 1979.
6. A.H. Sayed and T. Kailath, "A State-Space Approach to Adaptive RLS Filtering", IEEE Signal Processing Magazine, Jul. 1994.
7. M.E. Rollins and S.J. Simmons, "Error Performance Analysis of MLSE for Frequency-Selective Rayleigh Fading Channels with Kalman Channel Estimation", Proceedings of ICC '94, Vol. 1, pp. 312–326, 1994.
8. E.A. Lee and D.G. Messerschmitt, Digital Communication, Kluwer, second edition, 1994.

9. R.H. Clarke, "A Statistical Theory of Mobile-Radio Reception", Bell System Tech. J., Vol. 47, pp. 957–1000, 1968.
10. W.C. Jakes, Microwave Mobile Communications, Wiley, 1974.
11. G.A. Arredondo and W.H. Chriss, "A Multipath Fading Simulator for Mobile Radio", IEEE Transaction on Vehicular Technology, Vol. 22, pp. 241–244, Nov. 1973.
12. J.D. Parsons, The Mobile Radio Propagation Channel, Pentech Press, 1992.
13. S.M. Kay, Modern Spectral Estimation: Theory and Application, Prentice Hall, 1988.
14. J.G. Proakis, Digital Communications, McGraw-Hill, 3rd edition, 1995.
15. J.H. Lodge and M.J. Moher, "Maximum Likelihood Sequence Estimation of CPM Signals Transmitted over Rayleigh Flat-Fading Channels", IEEE Transaction on Communications, Vol. 38, pp. 787–794, Jun. 1990.
16. G.M. Vitetta and D.P. Taylor, "Maximum Likelihood Decoding of Uncoded and Coded PSK Signal Sequences Transmitted over Rayleigh Flat-Fading Channels", IEEE Transaction on Communications, Vol. 43, pp. 2750–2758, Nov. 1995.
17. P. Rao and M.A. Bayoumi, "An Efficient VLSI Implementation of Real-Time Kalman Filter", IEEE International Symposium on Circuit and Systems", Vol. 3, pp. 2353–2356, 1990.
18. P. Rao and M.A. Bayoumi, "An Algorithm Specific VLSI Parallel Architecture for Kalman Filter", VLSI Signal Processing IV, IEEE Press, pp. 264–273, 1991.
19. M.A. Bayoumi, P. Rao and B. Alhalabi, "VLSI Parallel Architecture for Kalman Filter an Algorithm Specific Approach", Journal of VLSI Signal Processing, Vol. 4, pp. 147–163, Kluwer Academic Publishers, 1992.

Mohammad Javad Omidi received his B.Eng. in Electronics, 1987, and M.A.Sc. in Communications, 1989, from Isfahan University of Technology, Isfahan, Iran. Currently, he is a Ph.D. candidate in the Department of Electrical Engineering, University of Toronto, where his research is focused on VLSI Implementation of Wireless Communication Algorithms.

S. Pasupathy was born in Chennai (Madras), Tamilnadu, India, on September 21, 1940. He received the B.E. degree in telecommunications from the University of Madras in 1963, the M.Tech. degree in electrical engineering from the Indian Institute of Technology, Madras, in 1966, and the M.Phil. and Ph.D. degree in engineering and applied science from Yale University in 1970 and 1972, respectively.

He jointed the faculty of the University of Toronto in 1973 and became a Professor of Electrical Engineering in 1983. He has served as the Chairman of the Communications Group and as the Associate Chairman of the Department of Electrical Engineering at the University of Toronto. His research interests are in the areas of communication theory, digital communications, and statistical signal processing. He is a registered Professional Engineer in the province of Ontario. During 1982–1989 he was an Editor for *Data Communications and Modulation* for the IEEE Transactions on Communications. He has also served as a Technical Associate Editor for the IEEE Communications Magazine (1979–1982) and as an Associate Editor for the *Canadian Electrical Engineering Journal* (1980–1983). Since 1984, he has been writing a regular column entitled "Light Traffic" for the IEEE Communications Magazine.

Dr. Pasupathy was elected as a Fellow of the IEEE in 1991 "for contributions to bandwidth efficient coding and modulation schemes in digital communication."

P. Glenn Gulak is a professor in the Department of Electrical and Computer Engineering at the University of Toronto. He is a senior member of the IEEE and a registered professional engineer in the province of Ontario.

His research interests are in the areas of circuits, algorithms and VLSI architectures for digital communications and signal processing applications. He has received several teaching awards for undergraduate courses taught in both the Department of Computer Science and the Department of Electrical and Computer Engineering at the University of Toronto.

Dr. Gulak received his Ph.D. from the University of Manitoba while holding a Natural Sciences and Engineering Research Council of Canada Postgraduate Scholarship. From 1985 to 1988 he was a research associate in the Information Systems Laboratory and the Computer Systems Laboratory at Stanford University. He has served on the ISSCC Signal Processing Technical Subcommittee since 1990 and currently serves as Program Secretary for ISSCC.